09

Effect of particle concentration on the dynamics of microcavities during the collision of 2π-unipolar pulses of self-induced transparency in a three-level medium

© R.M. Arkhipov, M.V. Arkhipov, N.N. Rozanov

Ioffe Institute,
St. Petersburg, Russia,

e-mail: arkhipovrostislav@gmail.com, mikhail.v.arkhipov@gmail.com, antpakhom@gmail.com, nnrosanov@mail.ru

Received October 22, 2024
Revised October 29, 2024
Accepted October 29, 2024

Based on the numerical solution of the system of material equations for the density matrix together with the wave equation for the electric field strength, the effect of the particle concentration of a three-level medium on the dynamics of microcavities during the collision of 2π-like unipolar attosecond pulses of self-induced transparency in a three-level medium is studied. The effect of changing the temporal shape of the pulses during propagation in a dense medium on the shape of the microcavities is also studied. It is shown that with increasing particle concentration the formation of microresonators is preserved, but their shape can be distorted.

Keywords:extremely short pulses, attosecond pulses, dynamic microcavities.

DOI: 10.61011/EOS.2024.11.60321.7162-24

1. Introduction

Over the past few years, nonlinear optics of unipolar half-cycle pulses has become a new, rapidly progressing area of modern physics and optics [1]. Numerous papers [2–14] and reviews [15–17] as well as monograph [18] have addressed this topic. Unipolar half-cycle pulses contain only one half-wave of electric field strength and therefore have extremely short duration in a given spectral range. For them, an important characteristic is the electrical area of the pulse, which is defined as the integral of the electric field strength E over time t at a given point in space r [19–21]:

$$S_E(r) = \int E(r,t)dt. \qquad (1)$$

The interest in half-cycle pulses is due to the ability to rapidly transfer mechanical momentum to an electron in one direction, making them promising for ultrafast control of the quantum system properties [22–26]. Currently the pulses with a well-defined half-wave field are available with duration in the attosecond range [2–14], which makes the optics of unipolar pulses an important part of modern attosecond physics [15–17]. Because of the short duration of such pulses (less than one field period), many new phenomena arise on such small time intervals that are impossible with conventional multi-cycle pulses of several field half-waves [1,15–17].

One of such phenomena is the recently predicted possibility of creating and ultrafast control of dynamic microcavities (MC) during the collision of unipolar half-cycle pulses in a resonant medium [27–32], see also a review [33]. The effect occurs during coherent interaction of pulses with the medium when their duration and the delays between them are shorter than the relaxation time of the medium polarisation T_2. In case of a simple two-level medium in the region of pulse overlap the population difference is almost constant. And outside of this area, it changes in a stepwise fashion and has another constant value or changes with the coordinate according to some law, i.e., a population difference lattice [34]. Such a structure represents an MC.

In [32] an analytical theory of the formation of such MCs in a multilevel medium in the approximations of a weak field (when perturbation theory is valid) and a sparse medium is presented. Numerical calculations carried out in a strong field and for a dense two-level medium when 2π-like Gaussian pulses of self-induced transparency (SIT) collide in it, have revealed a number of new features not predicted in the framework of a simple analytical model. These include the localisation of MC in the collision region of the pulses, the dependence of its shape on the initial polarity of the colliding pulses, etc. According to estimates, the Q-quality of such MCs can reach 10^4 at a significant concentration of atoms in the medium. Thus, the concentration of particles is an important parameter affecting the MC performance. Also, during coherent propagation of half-cycle SIT pulses in a dense medium, their shape can change [35,36]. In particular, the pulse may be split into sub-pulses, each of which will act on the medium as a SIT pulse.

In this study, the influence of the concentration of particles in the medium and the effect of changing the shape of SIT pulses on the MC dynamics during the collision of such pulses in a three-level medium are investigated. The case when Gaussian SIT pulses and hyperbolic secant pulses collide is considered. In both cases, a significant change in the shape of the MC as the concentration of particles

in the medium increases is revealed. The reflection of sample attosecond pulses from such structures can be used to study the ultrafast electron dynamics in solids [37] and other materials [38–40].

2. Theoretical model

The following system of equations for the density matrix of a three-level medium together with the wave equation describing the evolution of the electric field strength in the medium [41] was used in the following calculations:

$$\frac{\partial}{\partial t}\rho_{21} = -\rho_{21}/T_{21} - i\omega_{12}\rho_{21} - i\frac{d_{12}}{\hbar}E(\rho_{22}-\rho_{11}) - i\frac{d_{13}}{\hbar}E\rho_{23} + i\frac{d_{23}}{\hbar}E\rho_{31}, \quad (2)$$

$$\frac{\partial}{\partial t}\rho_{32} = -\rho_{32}/T_{32} - i\omega_{32}\rho_{32} - i\frac{d_{23}}{\hbar}E(\rho_{33}-\rho_{22}) - i\frac{d_{12}}{\hbar}E\rho_{31} + i\frac{d_{13}}{\hbar}E\rho_{21}, \quad (3)$$

$$\frac{\partial}{\partial t}\rho_{31} = -\rho_{31}/T_{31} - i\omega_{31}\rho_{31} - i\frac{d_{13}}{\hbar}E(\rho_{33}-\rho_{11}) - i\frac{d_{12}}{\hbar}E\rho_{32} + i\frac{d_{23}}{\hbar}E\rho_{21}, \quad (4)$$

$$\frac{\partial}{\partial t}\rho_{11} = \frac{\rho_{22}}{T_{22}} + \frac{\rho_{33}}{T_{33}} + i\frac{d_{12}}{\hbar}E(\rho_{21}-\rho_{21}^*) - i\frac{d_{13}}{\hbar}E(\rho_{13}-\rho_{13}^*), \quad (5)$$

$$\frac{\partial}{\partial t}\rho_{22} = -\rho_{22}/T_{22} - i\frac{d_{12}}{\hbar}E(\rho_{21}-\rho_{21}^*) - i\frac{d_{23}}{\hbar}E(\rho_{23}-\rho_{23}^*), \quad (6)$$

$$\frac{\partial}{\partial t}\rho_{33} = -\rho_{33}/T_{33} + i\frac{d_{13}}{\hbar}E(\rho_{13}-\rho_{13}^*) + i\frac{d_{23}}{\hbar}E(\rho_{23}-\rho_{23}^*), \quad (7)$$

$$P(z,t) = 2N_0 d_{12}\mathrm{Re}\rho_{12}(z,t) + 2N_0 d_{13}\mathrm{Re}\rho_{13}(z,t), \quad (8)$$

$$\frac{\partial^2 E(z,t)}{\partial z^2} - \frac{1}{c^2}\frac{\partial^2 E(z,t)}{\partial t^2} = \frac{4\pi}{c^2}\frac{\partial^2 P(z,t)}{\partial t^2}. \quad (9)$$

The following parameters are contained in this system of equations: $\hbar$ — the reduced Planck constant, N_0 — the concentration of particles, P — the polarisation of the medium, ω_{12}, ω_{32}, ω_{31} — the frequencies of resonance transitions, and d_{12}, d_{13}, d_{23} — the dipole moments of the transitions. The variables ρ_{11}, ρ_{22}, ρ_{33} — the populations of 1st, 2nd, and 3rd states of the medium, respectively, ρ_{21}, ρ_{32}, ρ_{31} — the off-diagonal elements of the density matrix determining the dynamics of the medium polarisation, and T_{ik} — -the relaxation times. System (2)–(9) was solved numerically. In calculations given below, the relaxation times are much longer than the durations of the processes under consideration and are not significant. The one-dimensional wave equation describes the propagation of unipolar pulses in coaxial waveguides [42].

3. Influence of propagation effects on the MC shape during coherent propagation of SIT pulses in a dense medium

In [43], an analytical solution of the system of Maxwell-Bloch equations was found for a two-level medium in the form of a unipolar soliton having the shape of a hyperbolic secant. Subsequently, this soliton was found in numerical and analytical calculations in [44–49] for two-level and multilevel media. In this section, we study the effect of shape change when a pair of SIT pulses in the form of a hyperbolic secant propagating towards each other from vacuum collide. The form of these colliding pulses travelling from left and right into the medium towards each other is given by:

$$E(z=0,t) = E_{01}\mathrm{sech}\left(\frac{t-6\tau}{\tau}\right)$$

$$E(z=L,t) = E_{02}\mathrm{sech}\left(\frac{t-6\tau}{\tau}\right) \quad (10)$$

In order for the pulse to act as a 2π SIT pulse at the 1–2 main transition of the medium (if the medium is two-level), the pulse amplitude must be expressed by the following relation [43]:

$$E_0 = \frac{\hbar}{d_{12}\tau} \quad (11)$$

Numerical calculations carried out in two-level [35] and three-level [36] media have shown a change in the shape of such a pulse during propagation, in particular the possibility of its splitting into sub-pulses.

The length of the whole integration region in the calculations, the results of which are given below, was $L = 15\lambda_0$. In this region the three-level medium was located between points $z_1 = 3\lambda_0$ and $z_2 = 12\lambda_0$. We numerically solved the system of equations (2)–(9) with the initial condition as two propagating toward each other half-cyclic pulses of opposite polarity $E_{01} = -E_{02} = 135570$ ESU and satisfied the condition (12), which corresponded to 2π-like SIT pulses. The pulse duration was$\tau = 388$ as. Parameters of the three-level medium: concentration of three-level particles: $N_0 = 2\cdot 10^{20}\,\mathrm{cm}^{-3}$, transition frequency 1–2 $\omega_{12} = 2.69\cdot 10^{15}$ rad/s (corresponding transition wavelength: $\lambda_{12} = \lambda_0 = 700$ nm), transition dipole moment: 1–2: $d_{12} = 20$ D, transition frequency: 1–3: $\omega_{13} = 1.5\omega_{12}$, transition dipole moment: $d_{13} = d_{12}/2$, transition frequency: $\omega_{23} = \omega_{13} - \omega_{12}$, transition dipole moment 2–3: $d_{23} = 0$. Relaxation times $T_{1k} = 1$ ns. The half-cycle pulses (10),(11) at the given parameters of the problem collided in the medium at the point with coordinate $z = z_c = 7.6\lambda_0$.

Coherent propagation of such pulses in the medium was not accompanied by a significant change in the pulse shape, but only a decrease in their amplitude with preservation of positive polarity. In this example, the pulses experienced a single collision in the medium. Figure 1 shows the spatiotemporal dynamics of the field strength of pulses 1 and 2 (propagation directions are shown by arrows) in the medium. The time dependence of the electric field $E(t)$ at the entrance to the medium, $z = 0$, (blue curve c) and at its exit, $z = L$, (orange line) is shown in Fig. 2. The dynamics of polarisation and population difference at each transition of the medium are shown in Fig. 3–6 respectively.

Fig. 4–6 shows the emergence of a thin channel at each transition of the medium. In the collision region the population difference has a constant value, and outside it changes in a stepwise manner, a localised MC appears in the medium in the region of pulse overlap. However, the shape of this MC changes with time and decays because of complex polarisation oscillations in a dense medium. If we increase the number of pulse collisions in the medium, the shape of the MC can change after each collision [20–24]. The MC dynamics at each transition of the medium for three collisions is shown in Fig. 7–9. To create a sequence of pulses at the boundary of the integration region, zero boundary conditions ('perfect mirrors') were used in the numerical calculations. The pulses leaving the medium reached the boundary of the integration region, were reflected from these mirrors and returned to the medium again, collided in it, and so on. The dynamics of the electric field is shown in Fig. 10. It can be seen that in these examples the microcavity shape hardly changes after each collision. This is due to the fact that the amplitude of the pulses decreased during propagation in the dense medium with distance. This can be seen in Fig. 2.

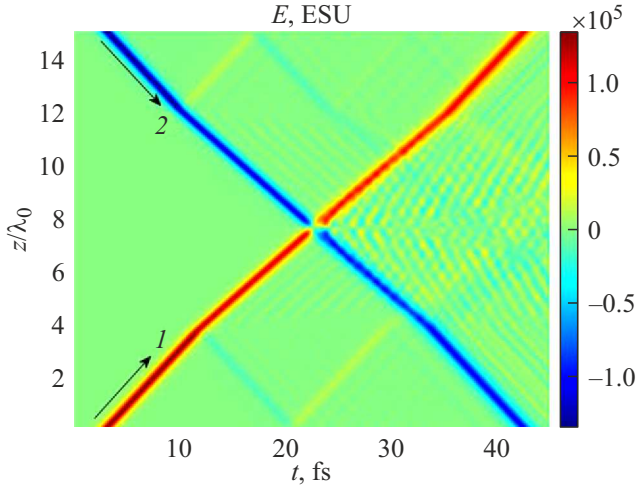

Figure 1. Spatiotemporal dynamics of the electric field $E(z,t)$ in a three-level medium.

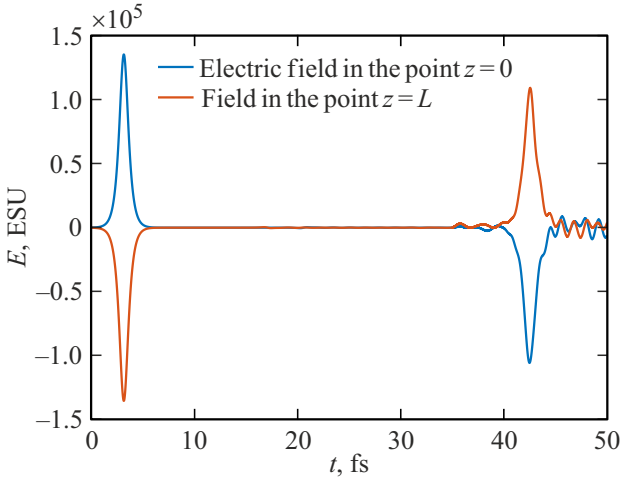

Figure 2. Time dependence of the electric field $E(t)$ at the entrance to the medium, $z = 0$(blue curve) and at its exit, $z = L$ (orange line).

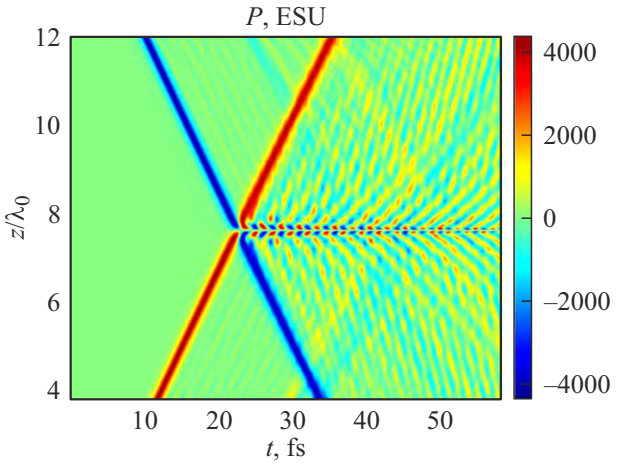

Figure 3. Spatiotemporal dynamics of the three-level medium polarisation P(z,t).

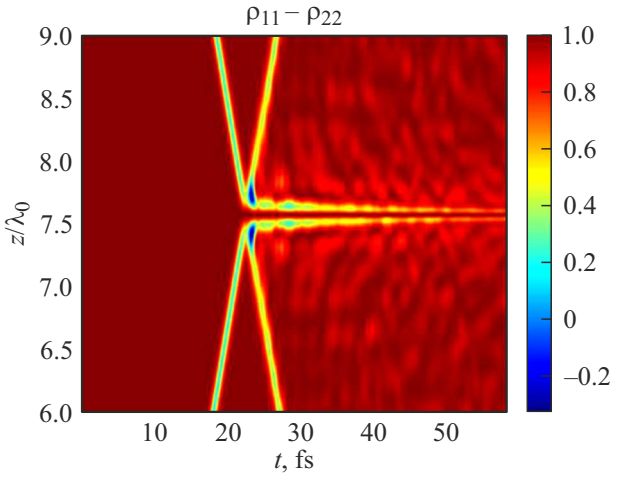

Figure 4. Spatiotemporal dynamics of the $\rho_{11} - \rho_{22}$ population difference of the three-level medium.

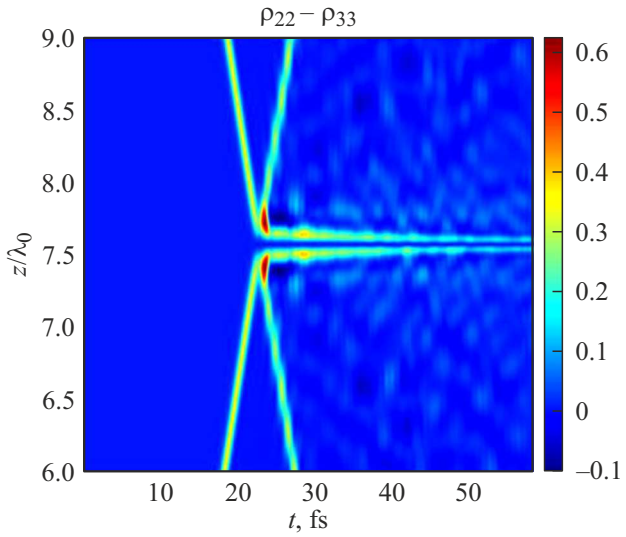

Figure 5. Spatiotemporal dynamics of the $\rho_{22} - \rho_{33}$ population difference of the three-level medium.

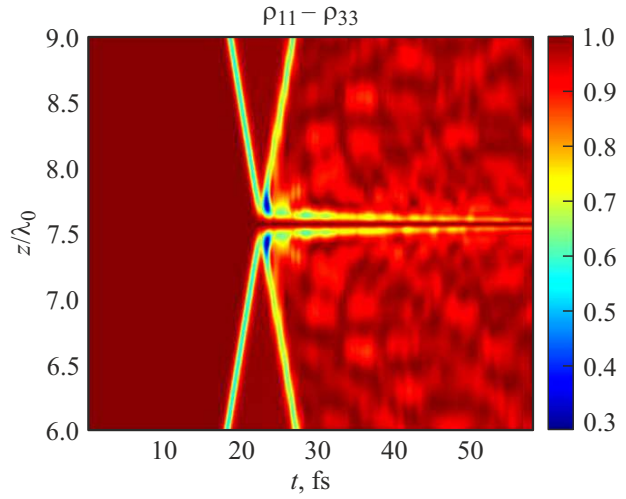

Figure 6. Spatiotemporal dynamics of the $\rho_{11} - \rho_{33}$ population difference of the three-level medium.

To solve this problem (decreasing the field amplitude during propagation in the absorbing medium), the losses can be compensated by amplification. To do this, one can use half-cyclic dissipative SIT solitons, which can be formed in a medium in which there is a mixture of active (amplifying) particles and passive (absorbing) atoms. The formation of such solitons has been shown theoretically in [45–48]. Their collision dynamics was studied in [50], in which the possibility of forming population lattices when such solitons collide in a single-mode light guide was shown.

In the previous example, the amplitude of the pulses was such that it acted similarly to a 2π-SIT pulse. In the following example, we will increase the amplitude of both pulses by a factor of 2 so that the pulse will act like a 4π-SIT pulse. When propagating in a three-level medium, such a pulse experiences splitting into a pair of unipolar pulses, each of which behaves like a 2π-like SIT pulse [27]. This splitting can be seen in Fig. 11, 12. The concentration value in this example was reduced by a factor of $N_0 = 10^{20}\,\mathrm{cm}^{-3}$. In these calculations, the pulse amplitude was increased by a factor of 2. The other parameters are the same as in Fig. 1–6.

Spatiotemporal dynamics of the population difference during a single pulse passage through the medium is shown in Fig. 13–15.

From these figures it follows that the microcavity is formed in the centre of the medium. But its shape is slightly blurred. In the next section, the MC dynamics during the collision of Gaussian pulses in the medium is considered.

It can be seen from the above figures that the induced structures change rapidly with time, with significant changes occurring over times of the order of 10 fs. Therefore, the reflection (diffraction) of a test pulse of the attosecond duration from such structures is preferable for studying ultrafast processes in matter. The dynamics of carriers in a solid body due to diffraction of an attosecond pulse

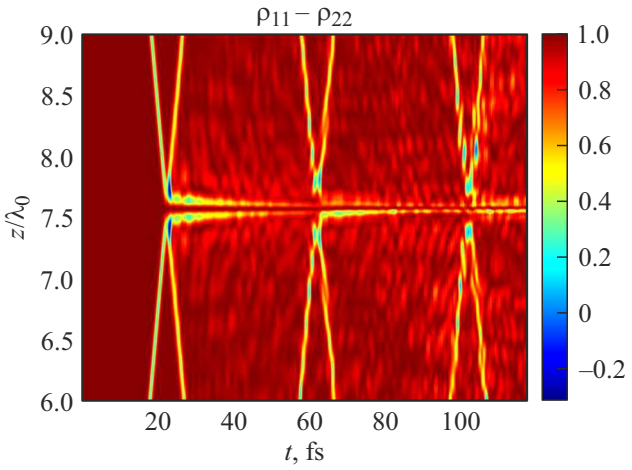

Figure 7. Spatiotemporal dynamics of the $\rho_{11} - \rho_{22}$ population difference of the three-level medium.

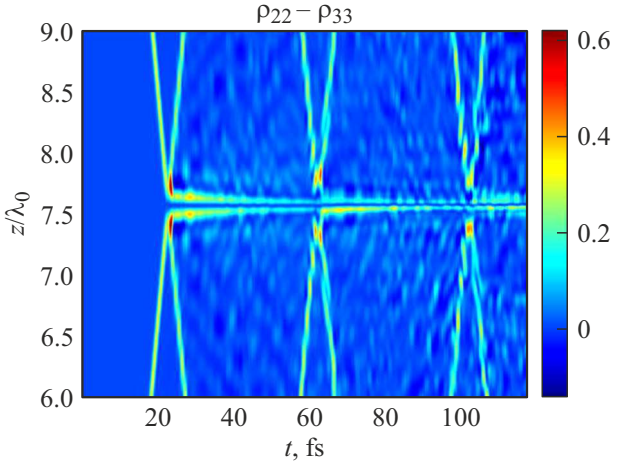

Figure 8. Spatiotemporal dynamics of the $\rho_{22} - \rho_{33}$ population difference of the three-level medium.

on atomic population lattices was experimentally studied in [28].

4. MC dynamics during collision of Gaussian pulses in a medium with increasing concentration of the medium

In the numerical calculations, the results of which are given in this section, the medium was excited by a sequence of oncoming half-cycle pulses having a Gaussian shape. At the initial moment of time, a pair of Gaussian pulses was sent into the medium towards each other from the left and at first

$$E_1(z=0,t) = E_{01}e^{-\frac{(t-\Delta_1)^2}{\tau^2}}, \quad (12)$$

$$E_2(z=L,t) = E_{02}e^{-\frac{(t-\Delta_2)^2}{\tau^2}}. \quad (13)$$

Here, $\Delta_1 = \Delta_2 = 2.5\tau$. A series of numerical calculations of the spatiotemporal dynamics of the population difference

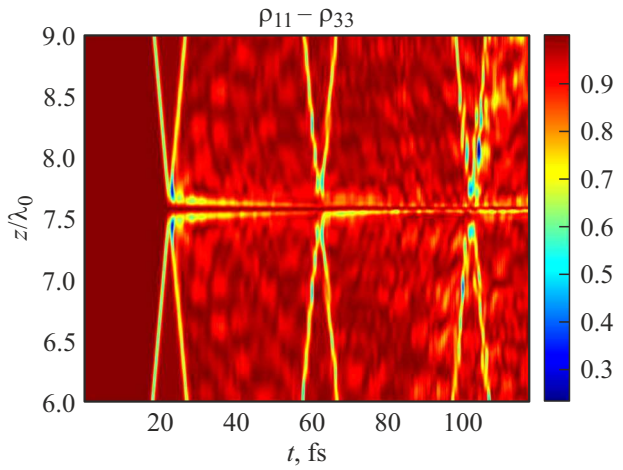

Figure 9. Spatiotemporal dynamics of the $\rho_{11} - \rho_{33}$ population difference of the three-level medium.

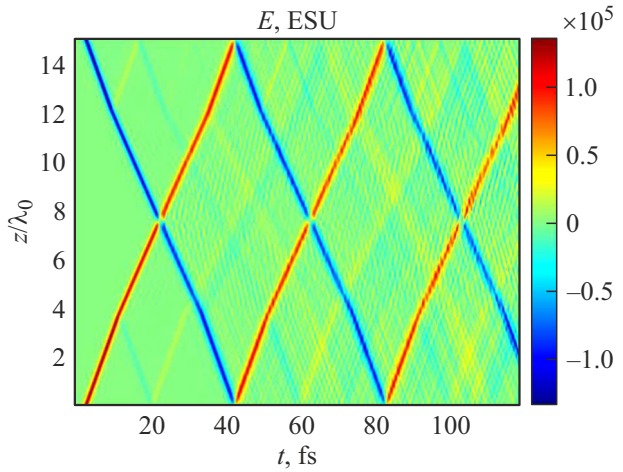

Figure 10. Spatiotemporal dynamics of the electric field $E(z,t)$.

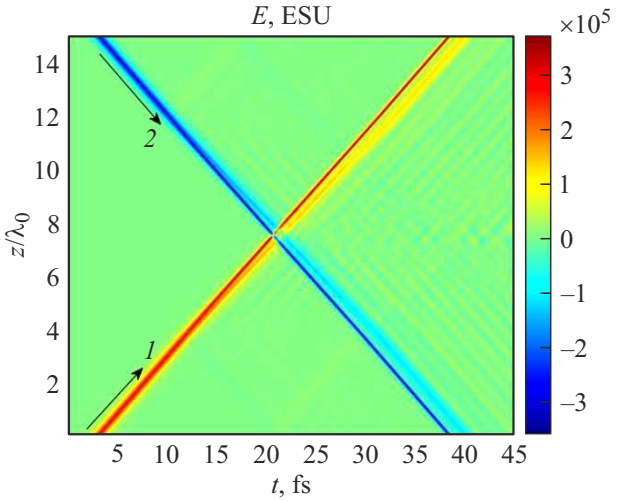

Figure 11. Spatiotemporal dynamics of the electric field $E(z,t)$ in a three-level medium.

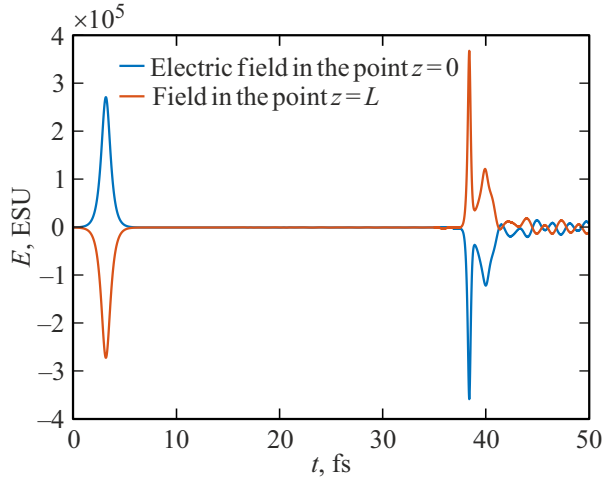

Figure 12. Time dependence of the electric field $E(t)$ at the entrance to the medium, $z = 0$(blue curve) and at its exit, $z = L$ (orange line).

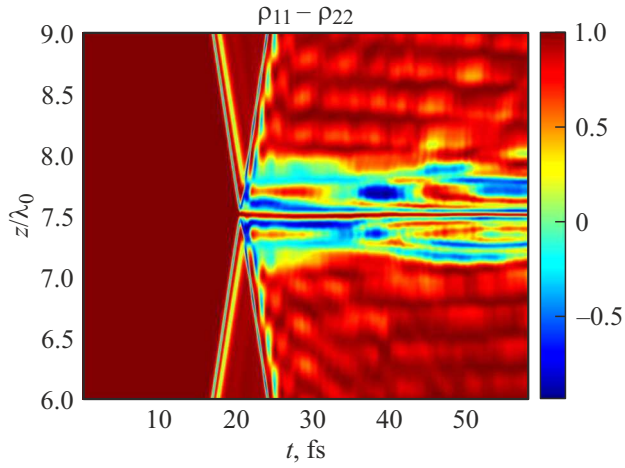

Figure 13. Spatiotemporal dynamics of the $\rho_{11} - \rho_{22}$ population difference of the three-level medium.

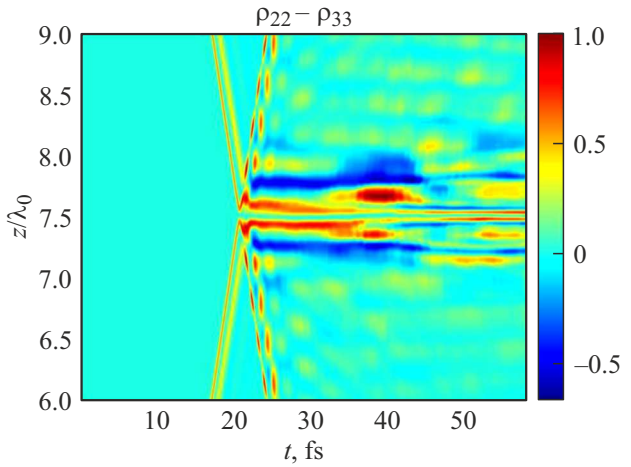

Figure 14. Spatiotemporal dynamics of the $\rho_{22} - \rho_{33}$ population difference of the three-level medium.

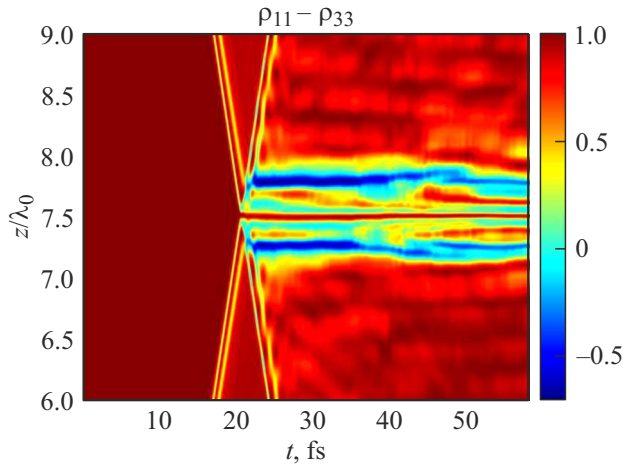

Figure 15. Spatiotemporal dynamics of the $\rho_{11} - \rho_{33}$ population difference of the three-level medium.

at different values of the medium particle concentration were carried out. The amplitude of the pulses was $E_{01} = -E_{01} = 175000$ ESU. The pulse amplitude was chosen so that the pulses act like SIT pulses for the $1-2$ transition of the medium. Pulse duration: $\tau = 777$ as. Parameters of the three-level medium: $1-2$: $\omega_{12} = 2.69 \cdot 10^{15}$ rad/s (corresponding transition wavelength: $\lambda_{12} = \lambda_0 = 700$ nm), transition dipole moment: $1-2$: $d_{12} = 20$ D, transition frequency: $1-3$: $\omega_{13} = 1.7\omega_{12}$, transition dipole moment: $d_{13} = 0$, transition frequency: $\omega_{23} = \omega_{13} - \omega_{12}$, transition dipole moment $2-3$: $d_{23} = 1.5d_{12}$. Relaxation times. $T_{1k} = 1$ ns. The difference of relaxation times for different levels is not fundamental because the duration of the considered processes is much shorter than the relaxation times. The concentration of three-level medium particles was a variable parameter.

Figures 16, $a-18$, a illustrate the dynamics of the population difference at each medium transition at $N_0 = 10^{19}$ cm^{-3} as a result of five pulse collisions in the medium. The instantaneous distribution of the population difference in space after the first collision is shown in Fig. 16, $b-18$, b. The pulses in these examples collide at the point $z_c = 6\lambda_0$. Since the pulses have opposite polarity, in the vicinity of the collision point the field strength is close to zero and the medium is not excited. And at the edges of this region, a lattice of populations of several periods appears. Thus, an MC localised in the region of pulse overlap appears. Similar structures have been observed during the collision of SIT pulses in a two-level [35].

The spatiotemporal dynamics of the population difference at the main transition $1-2$ is shown in Fig. 19, a at $N_0 = 5 \cdot 10^{19}$ cm^{-3} and in Fig. 19, b at $N_0 = 10^{20}$ cm^{-3}.

Similar dynamics is observed at other resonance transitions of the medium. These figures show that the MC is preserved in the dense medium as well. As the number of collisions increases, the number of periods in the lattice increases, as in the two-level medium [26]. From Fig. 19, ,b, an important result of MC preservation at concentration $N_0 = 10^{20}$ cm^{-3} follows. As shown in [26], the MC Q-quality at such large concentrations can reach $10-1000$ in a dense medium. However, the Q-quality in this study was evaluated in the stationary lattice approximation. In our case, the structures are dynamic — they change with time and exist on times of the order of the phase memory time of the medium T_2. Therefore, the above estimates are valid on timescales smaller than this time.

Conclusion

In this paper, the formation and control of dynamic microcavities during the collision of unipolar pulses of two types: Gaussian and in the form of hyperbolic secant in a three-level dense medium when the density of the medium is varied has been studied based on numerical calculations. The initial pulses had opposite polarity. The pulse parameters were chosen so that the pulses acted similarly to 2π- and 4π-SIT pulses on the main transition of the medium.

It is shown that in the case of collision of 2π-like pulses in the form of a hyperbolic secant the formation of MC occurs, the shape of which hardly changes as the number of collisions between the pulses increases. Only a decay of the amplitude of the population equality occurs. This is due to the pulse amplitude decrease during propagation. To solve this problem, dissipative SIT solitons can be used to create an MC [45–48]. In case of collision of 4π-like pulses in the form of a hyperbolic secant, when the pulse propagates in a dense medium, it splits into a pair of 2π-like half-cycle SIT pulses. However, this also results in the formation of MC with smeared boundaries. The MC behaviour at collision of Gaussian 2π-like SIT half-cycle pulses in a three-level medium at different values of particle concentration was

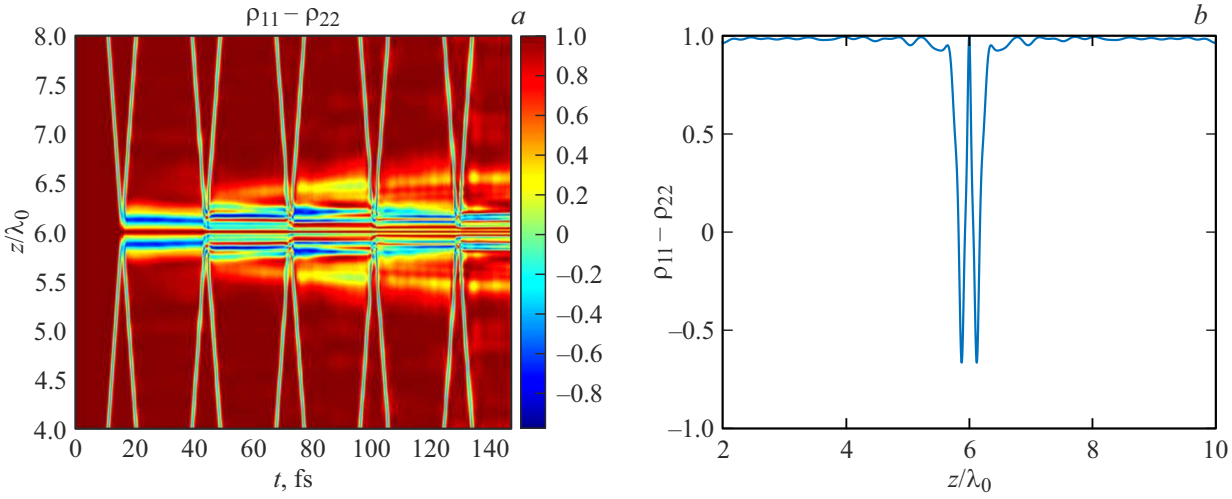

Figure 16. Spatiotemporal dynamics of the population difference $\rho_{11} - \rho_{22}$ of the three-level medium (a) and the cross section of this dependence at $t = 30$ fs (b), $N_0 = 10^{19}$ cm^{-3}.

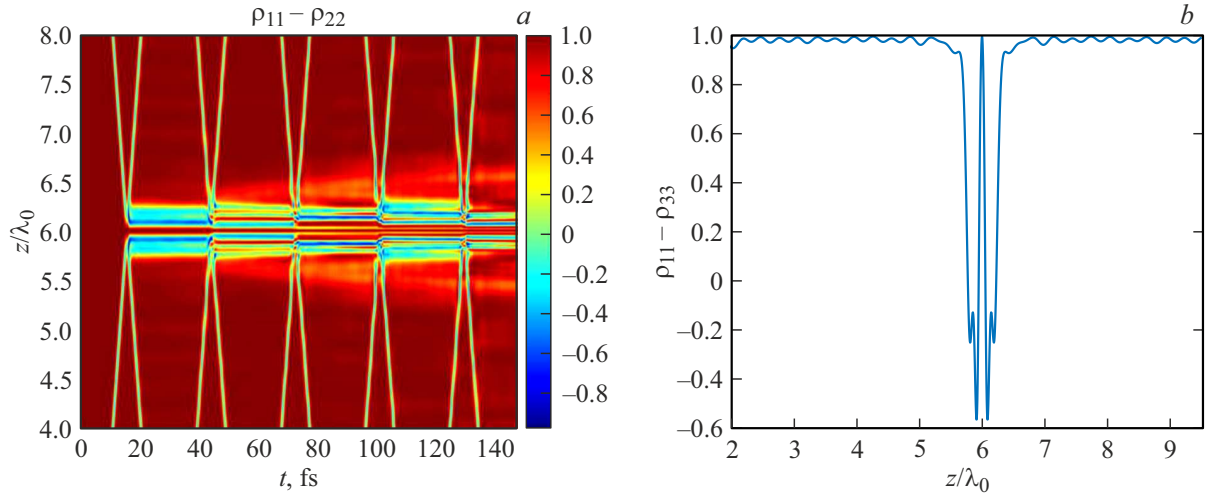

Figure 17. Spatiotemporal dynamics of the population difference $\rho_{11} - \rho_{33}$ of the three-level medium (a) and the cross section of this dependence at $t = 30$ fs (b), $N_0 = 10^{19}$ cm^{-3}.

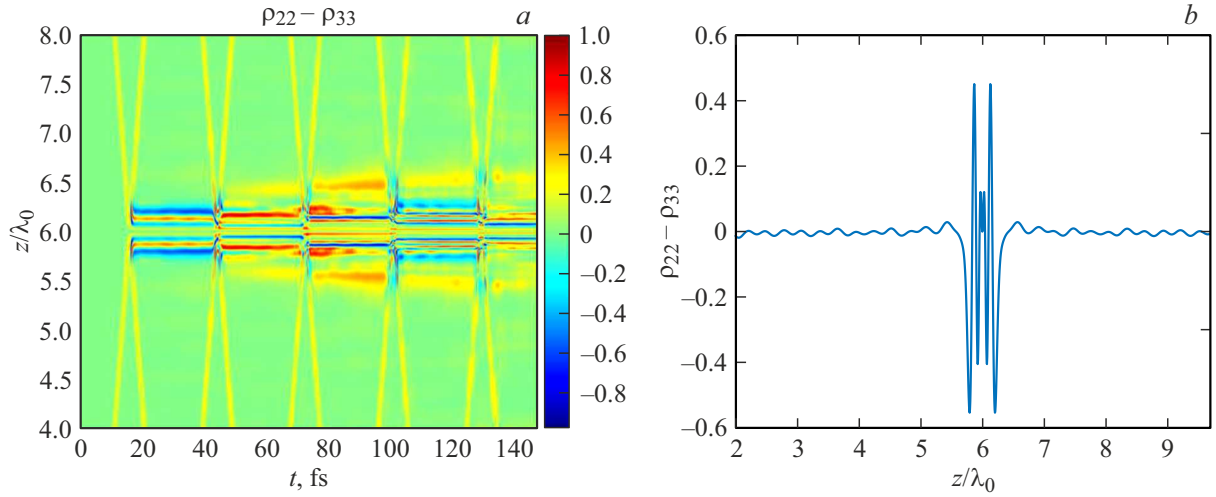

Figure 18. Spatiotemporal dynamics of the population difference $\rho_{22} - \rho_{33}$ of the three-level medium (a) and the cross section of this dependence at $t = 30$ fs (b), $N_0 = 10^{19}$ cm^{-3}.

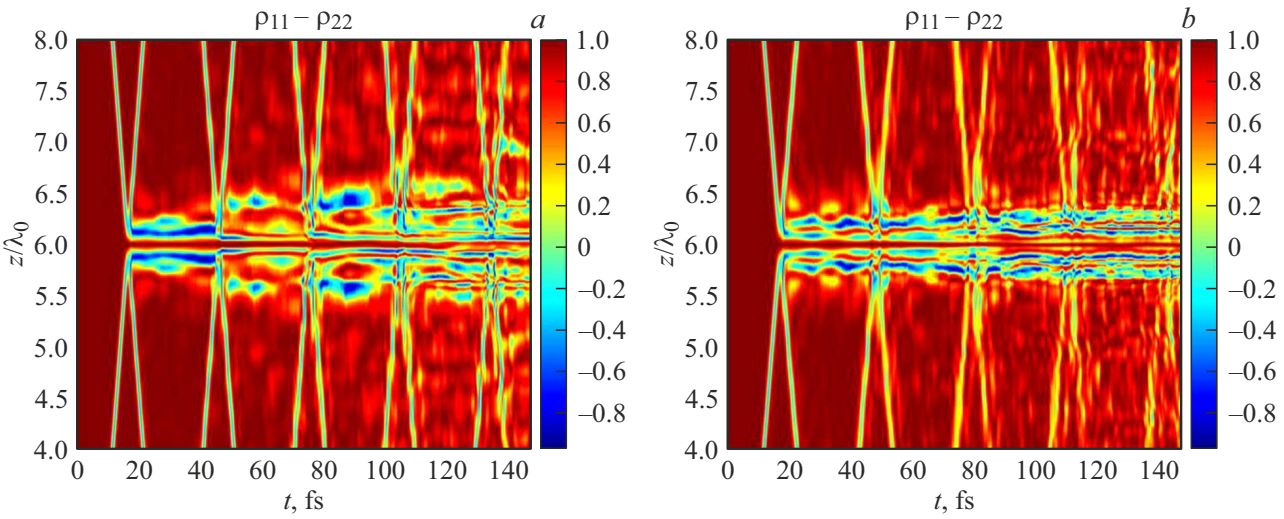

Figure 19. The spatiotemporal dynamics of the population difference $\rho_{11}-\rho_{22}$ of the three-level medium, $N_0 = 5 \cdot 10^{19}\,\mathrm{cm}^{-3}$ (*a*), $N_0 = 10^{20}\,\mathrm{cm}^{-3}$ (*b*).

also investigated. The results of these calculations showed that MCs can be formed in a dense medium.

The structures considered in this study provide new areas of research in studying ultrafast processes in matter during reflection of attosecond pulses from such structures [37–40], in the physics of space-time photonic crystals [51] and ultrafast optics for creating attosecond switching of the medium state [52].

Funding

The research was financially supported by the Russian Science Foundation under the scientific project 23-12-00012 (section 3) and by the state order of the A.F. Ioffe Institute of Physics and Technology, topic 0040-2019-0017 (section 4).

Conflict of interest

The authors declare that they have no conflict of interest.

References

[1] R.M. Arkhipov, M.V. Arkhipov, N.N. Rosanov. Quant. Electron., **50** (9), 801 (2020).
[2] M.T. Hassan, T.T. Luu, A. Moulet, O. Raskazovskaya, P. Zhokhov, M. Garg, N. Karpowicz, A.M. Zheltikov, V. Pervak, F. Krausz, E. Goulielmakis. Nature, **530**, 66 (2016).
[3] R.M. Arkhipov. Opt. Spectrosc., **120**, 756 (2016).
[4] H.-C. Wu, J. Meyer-ter Vehn. Nature Photon., **6**, 304 (2012).
[5] J. Xu, B. Shen, X. Zhang, Y. Shi, L. Ji, L. Zhang, T. Xu, W. Wang, X. Zhao, Z. Xu. Sci. Rep., **8**, 2669 (2018).
[6] S.V. Sazonov. JETP Lett., **114** (3), 132 (2021).
[7] M.M. Glazov, N.N. Rosanov. Phys. Rev. A, **109** (5), 053523 (2024).
[8] A.V. Bogatskaya, E.A. Volkova, A.M. Popov. Phys. Rev. E, **105**, 055203 (2022).
[9] E. Ilyakov, B.V. Shishkin, E.S. Efimenko, S.B. Bodrov, M.I. Bakunov. Opt. Express, **30**, 14978 (2022).
[10] A.S. Kuratov, A.V. Brantov, V.F. Kovalev, V.Yu. Bychenkov. Phys. Rev. E, **106**, 035201 (2022).
[11] N.N. Rosanov. Opt. Lett., **49** (6), 1493 (2024).
[12] S. Wei, Y. Wang, X. Yan, B. Eliasson. Phys. Rev. E, **106**, 025203 (2022).
[13] Q. Xin, Y. Wang, X. Yan, B. Eliasson. Phys. Rev. E, **107**, 035201 (2023).
[14] H. Dang, J. Gao, H. Wu, X. Guo, Y.R. Shen, L. Tong. arXiv preprint arXiv:2408.07306, (2024).
[15] N.N. Rosanov. Phys. Usp., **66**, 1059 (2023).
[16] N.N. Rosanov, M.V. Arkhipov, R.M. Arkhipov, A.V. Pakhomov. Contemprorary Physics, **64** (3), 224 (2023).
[17] N.N. Rosanov, M.V. Arkhipov, R.M. Arkhipov, Phys. Usp., **67** (11) (2024). DOI: 10.3367/UFNe.2024.07.039718.
[18] N.N. Rozanov, M.V. Arkhipov, A.V. Pakhomov, Kollektivnaya monografiya „Teragertsovaya fotonika“ Ed. by V.Ya. Panchenko, A.P. Shkurinov (Russian Academy of Sciences, M., 2023), p. 360–393.
[19] J.D. Jackson. Classical Electrodynamics (J. Willey, NY., 1962).
[20] E.G. Bessonov. Sov. Phys. JETP, **53**, 433 (1981).
[21] N.N. Rosanov. Opt. Spectrosc., **107**, 721 (2009).
[22] P.H. Bucksbaum. AIP Conference Proceedings, **323** (1), 416–433. (1994).
[23] A.S. Moskalenko, Z.-G. Zhu, J. Berakdar. Phys. Rep., **672**, 1 (2017).
[24] N. Rosanov, D. Tumakov, M. Arkhipov, R. Arkhipov. Phys. Rev. A, **104** (6), 063101 (2021).
[25] A. Pakhomov, M. Arkhipov, N. Rosanov, R. Arkhipov. Phys. Rev. A, **105**, 043103 (2022).
[26] R. Arkhipov, P. Belov, A. Pakhomov, M. Arkhipov, N. Rosanov. JOSA B, **41** (1), 285 (2024).
[27] O.O. Diachkova, R.M. Arkhipov, M.V. Arkhipov, A.V. Pakhomov, N.N. Rosanov. Opt. Commun., **538**, 129475 (2023).
[28] O. Diachkova, R. Arkhipov, A. Pakhomov, N. Rosanov. Opt. Commun., **565**, 130666 (2024).
[29] R. Arkhipov, A. Pakhomov, O. Diachkova, M. Arkhipov, N. Rosanov. Opt. Lett., **49** (10), 2549–2552 (2024).

[30] R.M. Arkhipov. Bulletin of the Lebedev Physics Institute, **51** (5), S366 (2024).
[31] R.M. Arkhipov, N.N. Rosanov. Opt. i spektr., **132** (5), 532 (2024) (in Russian).
[32] R. Arkhipov, A. Pakhomov, O. Diachkova, M. Arkhipov, N. Rosanov. J. Opt. Soc. Am. B., **41** (8), 1721 (2024).
[33] R.M. Arkhipov, O. Diachkova, M.V. Arkhipov, A. Pakhomov, N.N. Rosanov. Opt. i spektr., **132** (9) (2024).
[34] R.M. Arkhipov, M.V. Arkhipov, I. Babushkin, A. Demircan, U. Morgner, N.N. Rosanov. Opt. Lett., **41**, 4983 (2016).
[35] R. Arkhipov, M. Arkhipov, I. Babushkin, A. Pakhomov, N. Rosanov. JOSA B, **38** (6), 2004 (2021).
[36] R.M. Arkhipov, M.V. Arkhipov, N. Rosanov. ZHETF, **166** (8), 274 (2024). (IN RUSSIAN)
[37] R. Quintero-Bermudez, L. Drescher, V. Eggers, K.G. Xiong, S.R. Leone. arXiv preprint arXiv:2407.19609 (2024).
[38] H.J.B. Marroux, S. Polishchuk, O. Cannelli, R.A. Ingle, G.F. Mancini, C. Bacellar, M. Puppin, R. Geneaux, G. Knopp, L. Foglia, J. Phys. B: At. Mol. Opt. Phys., **57** 115401 (2024).
[39] U. Choudhry, T. Kim, M. Adams, J. Ranasinghe, R. Yang, B. Liao. J. Appl. Phys., **130** (2021).
[40] H.J. Eichler, P. Günter, D.W. Pohl. Laser-Induced Dynamic Gratings (Springer, Berlin, 1986), vol. 50.
[41] A. Yariv. Quantum Electronics (Wiley, NY., 1975).
[42] N.N. Rosanov. Opt. Spectrosc., **127**, 1050 (2019).
[43] R.K. Bullough, F. Ahmad. Phys. Rev. Lett., **27**, 330 (1971).
[44] V.P. Kalosha, J. Herrmann. Phys. Rev. Lett., **83**, 544 (1999).
[45] N.V. Vysotina, N.N. Rozanov, V.E. Semenov. JETP Lett., 83 (7), 279 (2006).
[46] N.N. Rosanov, V.E. Semenov, N.V. Vysotina. Quantum. Electron., **38**, 137 (2008).
[47] N.V. Vysotina, N.N. Rosanov, V.E. Semenov. Opt. Spectrosc., **106**, 713 (2009).
[48] N.N. Rosanov. *Dissipativnye opticheskie solitony. Ot mikro-k nano-i atto* (Fizmatlit, M., 2011) chapter 17. (in Russian).
[49] A.Y. Parkhomenko, S.V. Sazonov, JETP, **87** (5), 864 (1998).
[50] N.N. Rosanov, V.E. Semenov, N.V. Vyssotina. Laser Phys., **17**, 1311 (2007).
[51] Y. Sharabi, A. Dikopoltsev, E. Lustig, Y. Lumer, M. Segev. Optica, **9** (6), 585–592 (2022).
[52] M.T. Hassan. ACS Photonics, **11**, 334–338 (2024).

Translated by J.Savelyeva